

MOF-Derived Nanocobalt for Oxidative Functionalization of Cyclic Amines to Quinazolinones with 2-Aminoarylmethanols

Feng Xie, Qinghua Chen, Rong Xie, Huanfeng Jiang, and Min Zhang

ACS Catal., Just Accepted Manuscript • DOI: 10.1021/acscatal.8b01366 • Publication Date (Web): 25 May 2018

Downloaded from <http://pubs.acs.org> on May 25, 2018

Just Accepted

“Just Accepted” manuscripts have been peer-reviewed and accepted for publication. They are posted online prior to technical editing, formatting for publication and author proofing. The American Chemical Society provides “Just Accepted” as a service to the research community to expedite the dissemination of scientific material as soon as possible after acceptance. “Just Accepted” manuscripts appear in full in PDF format accompanied by an HTML abstract. “Just Accepted” manuscripts have been fully peer reviewed, but should not be considered the official version of record. They are citable by the Digital Object Identifier (DOI®). “Just Accepted” is an optional service offered to authors. Therefore, the “Just Accepted” Web site may not include all articles that will be published in the journal. After a manuscript is technically edited and formatted, it will be removed from the “Just Accepted” Web site and published as an ASAP article. Note that technical editing may introduce minor changes to the manuscript text and/or graphics which could affect content, and all legal disclaimers and ethical guidelines that apply to the journal pertain. ACS cannot be held responsible for errors or consequences arising from the use of information contained in these “Just Accepted” manuscripts.



MOF-Derived Nanocobalt for Oxidative Functionalization of Cyclic Amines to Quinazolinones with 2-Aminoarylmethanols

Feng Xie, Qing-Hua Chen, Rong Xie, Huan-Feng Jiang, and Min Zhang*

Key Lab of Functional Molecular Engineering of Guangdong Province, School of Chemistry and Chemical Engineering, South China University of Technology, Guangzhou 510641, People's Republic of China

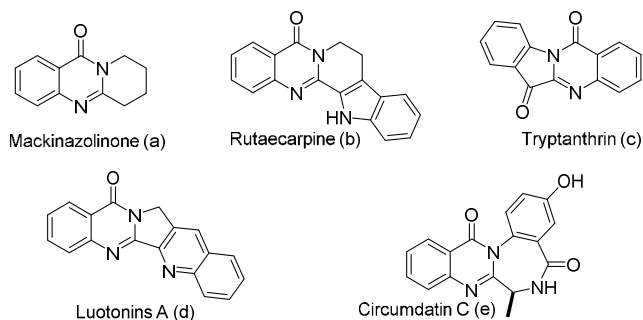
ABSTRACT: By employing a MOF-templated method, we have developed a highly dispersed and ultralow loading cobalt nanocatalyst, which has been applied in the oxidative functionalization of easily available cyclic amines with 2-aminoarylmethanols to ring-fused quinazolinones, the core structures of numerous valuable products. The developed catalytic transformation proceeds with the merits of broad substrate scope, good functional group tolerance and chemoselectivity, high step- and atom-efficiency, use of natural abundant Co/O₂ system, which offers a practical way for the preparation of quinazolinones with structural diversity. The work presented has built an important basis for direct conversion of cyclic amine motifs into functional frameworks.

KEYWORDS: heterogeneous nanocatalyst, cobalt, MOF-templated method, dehydrogenative coupling, quinazolinones

Cyclic amines represent a class of bulk chemical raw materials, and the related structural units extensively exist in numerous natural products, bioactive molecules, pharmaceuticals, agrochemicals, and functional materials. Consequently, the development of new strategies for direct transformation of cyclic amine motifs into functionalized frameworks is of significant importance,¹ as it offers the potential to lead to the discovery of new products with original biological and physical properties. Over the past decade, considerable attention has been directed towards the full dehydrogenation of cyclic amines into N-heteroarenes by developing alternative catalyst systems.² However, the creation of functionalized N-heteroarenes, by utilizing the initially dehydrogenated cyclic amines as the coupling agents for the next step of a given sequence, remains a new subject to be explored. Ideally, such a strategy would benefit from streamline synthesis of functional products that need multistep synthetic procedures with the conventional routes.

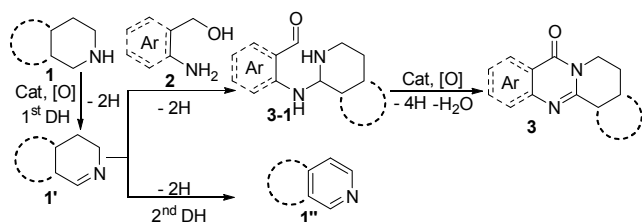
Ring-fused quinazolinones constitute the core structures of many natural alkaloids and manmade compounds that exhibit interesting biological and therapeutic activities,³ such as anti-depressant (Scheme 1, a),^{4a} antithrombotic activity (b),^{4b} anti-inflammatory (c),^{4c} anticancer (d)^{4d} and radical-scavenging (e) ones.^{4e} Furthermore, quinazolinones are characteristic of multiple sites with high affinity, which contribute to the development of medicinally relevant products.⁵ In general, quinazolinones are prepared via the cyclocondensation of anthranilamides with aldehydes or its surrogates.⁶ In addition, a number of new approaches have also been nicely explored to access the related scaffolds in recent years. Representative examples mainly involve carbonylative annulation reactions,⁷ the initial C-N bond formation of 2-halobenzoic acid followed by intramolecular cyclocondensation,⁸ the oxidative cyclization of anthranilamide derivatives,⁹ the oxidation of indoles followed by ring-expansion process,¹⁰ and the radical-induced cascade reactions.¹¹ Despite the significant utility of these achievements, most of them suffer from one or more drawbacks such as the use of less environmentally benign

oxidants and coupling agents, multistep procedures to access reactants and difficult catalyst reusability. Hence, the exploration of new methods for straightforward synthesis of ring-fused quinazolinones from easily available reagents with recyclable catalysts, preferably earth-abundant metals, still remains a highly demanding goal.



Scheme 1. Representative Quinazolinone Alkaloids

As a part of our sustained efforts towards the construction of N-heterocycles by hydrogen transfer¹² and dehydrogenation-mediated coupling strategies,¹³ we were inspired to develop a new protocol for the synthesis of ring-fused quinazolinones **3** from easily available cyclic amines **1** with the electron-rich 2-aminoarylmethanols **2**. As illustrated in Scheme 2, the first dehydrogenation of **1** forms imine **1'**, and the amino group of **2** would be able to undergo nucleophilic addition to **1'** and form amination **3-1**. Then, product **3** is afforded via the intramolecular oxidative coupling of **3-1**. However, it is important to note that the second dehydrogenation of **1'** to the non-coupling N-heteroarene **1''** is a thermodynamically favorable process. So, to achieve chemo-selective synthesis of product **3**, there should be a compatible system to ensure that the dehydrogenation rate of **1** is slow enough, thus favoring the capture of **1'** by amine **2**.



Scheme 2. Envisioned New Strategy

The aforementioned information led us to envisage that the development of a low-loading heterogeneous catalyst would offer a key to address the existing issue. As such a catalyst is different from the homogeneous ones, it exhibits low dehydrogenation efficiency due to the low density of catalytic sites and the occurrence of reactions on the solid surface. In recent years, the metal nanomaterials supported on nitrogen-doped carbon by utilizing metal-organic frameworks (MOFs) as the sacrificial templates have attracted much attention.¹⁴ This unique route benefits from the high specific surface area, tunable pore volumes and active sites of the resulting materials, which make them as single-site catalysts presenting specific activity.¹⁵ Moreover, the earth-abundant cobalt has been utilized to develop heterogeneous catalysts, which show impressive catalytic performance toward the well-known hydrogenation and dehydrogenation processes.¹⁶ However, their applications in the development of novel and challenging organic transformations remain scarcely explored. Herein, we report the preparation and characterization of a new cobalt nanocatalyst supported on N-doped carbon via a MOF-templated method, and described, for the first time, its utility in straightforward synthesis of ring-fused quinazolinones from cyclic amines and 2-aminoaryl methanols.

Typically, the cobalt heterogeneous catalyst was prepared by direct pyrolysis of MOF templates.¹⁷ Initially, the UiO-66-NH₂ MOFs were assembled in DMF from ZrCl₄ and organic linker 2-aminoterephthalic acid (H₂BDC-NH₂), then the metal precursor Co(NO₃)₂·6H₂O and ligand 1,4-diazabicyclo[2.2.2]octane (DABCO) were introduced into the MOFs via an *in situ* impregnating method. The uncombined amine group and DABCO as anchoring sites coordinated with the Co ion to prevent cobalt from the aggregation during the pyrolysis process. Finally, the resulting composites were pyrolyzed under argon flow at 800 °C for 3 h, which afforded the cobalt nanoparticles supported on the nitrogen-doped carbon (denoted as Co-ZrO₂/N-C, for more details see the Supporting Information (SI)).

The XRD pattern of the Co-ZrO₂/N-C (Figure S1 in the SI) just displays characteristic peaks of cubic and monoclinic ZrO₂, and no other peaks ascribing to the cobalt metal or its related compounds were observed, which indicates that the cobalt species are highly dispersed or amorphous. The N₂ adsorption-desorption isotherms of Co-ZrO₂/N-C exhibits a typical I isotherm (Figure S2), suggesting the existence of micro-mesoporous structure. Moreover, the BET specific surface area is shown to be 436 m²g⁻¹. The corresponding distribution of the pore diameters is in the range from 0.5-3.5 nm (Figure S2), the dominant pore size is centered at 0.6-0.8 nm (micropore) and 2.5-2.7 nm (mesopore), this unique micro-mesoporous structure makes for overcoming the mass transfer resistance and favors the substrate diffusion.

Further structural characterization was investigated by means of TEM, HRTEM and EDS analyses. The TEM image (Figure 1a) as well as HRTEM (Figure S3a-3c, SI) demonstrates the existence of two different crystal phases of Zr nanoparticles, but fails to show individual Co clusters, suggesting that the cobalt nanoparticles are uniformly dispersed, which is in good agreement with the XRD results. Furthermore, as shown in STEM image (Figure 1b) and corresponding elemental mapping results (Figure 1c-1d, Figure S4), the signals of Co, Zr, N, C, O are highly overlapped and interconnected with each other, and the Co nanoparticles are embedded in the N-doped carbon matrix, which are the results of utilizing MOF-templated method that leads to no cobalt agglomeration during pyrolysis process.

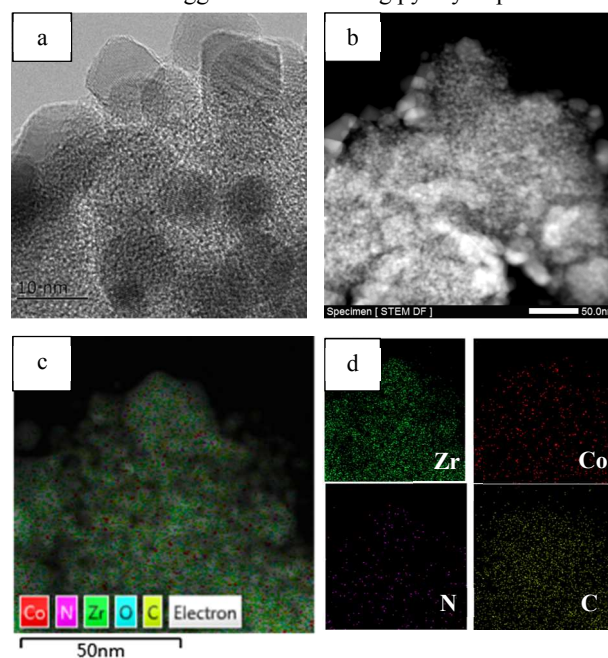


Figure 1. (a) TEM images of Co-ZrO₂/N-C. (b) STEM image of Co-ZrO₂/N-C. (c,d) EDS elemental maps of combined image, Zr, Co, N, C.

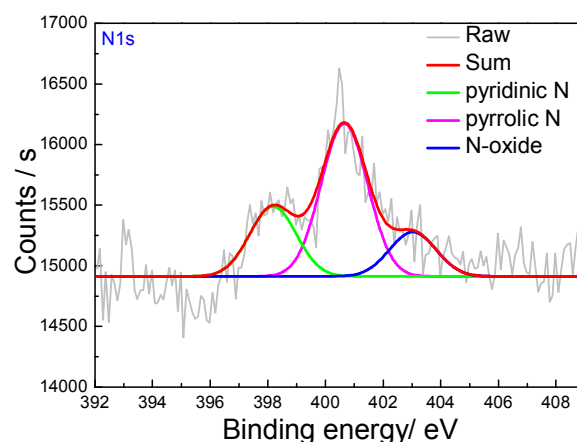
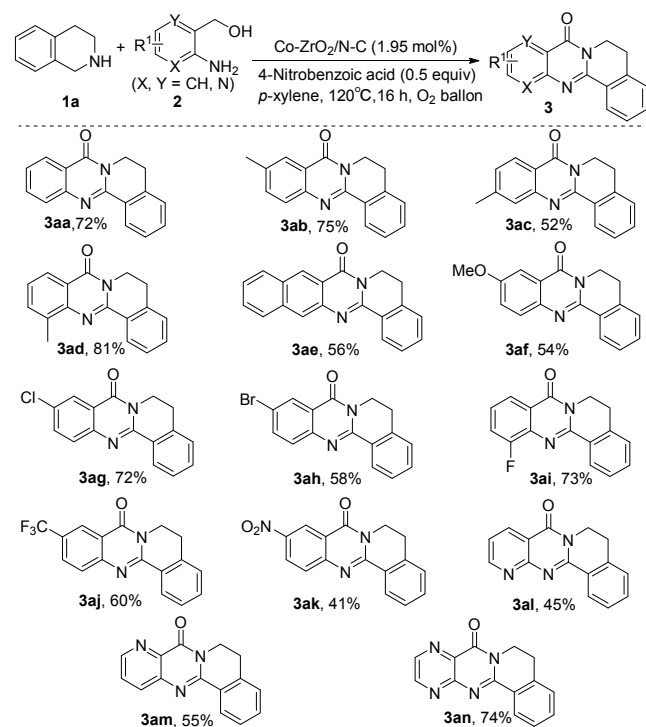


Figure 2. N1s XPS spectra of Co-ZrO₂/N-C.

X-ray photoelectron spectroscopy (XPS) was subsequently performed to study the surface chemistry of Co-ZrO₂/N-C. The element contents on the surface are as follows: Co (0.45 wt%), Zr (37.6 wt%), N (2.65 wt%), O (22.5 wt%) and C

(36.8 wt%). Meanwhile, an ultralow loading of Co was determined by ICP-AES (0.32 wt%). The N 1s spectrum (Figure 2) could be deconvoluted into three peaks with pyridinic N (398.4 eV), pyrrolic N (400.7 eV) and N-oxide species (403 eV).^{18a-c} The pyridinic N and pyrrolic N contribute to coordination with Co. Similarly, the Zr 3d spectrum (Figure S5b in SI) shows two evident peaks at 181.92 and 184.28 eV, which are the signals of ZrO₂.^{18d} The ultralow concentration of Co results in a very weak peak in Co 2p spectrum (Figure S5c) with binding energy of 781.9 eV, which is assigned to the Co-N_x species.^{18b}

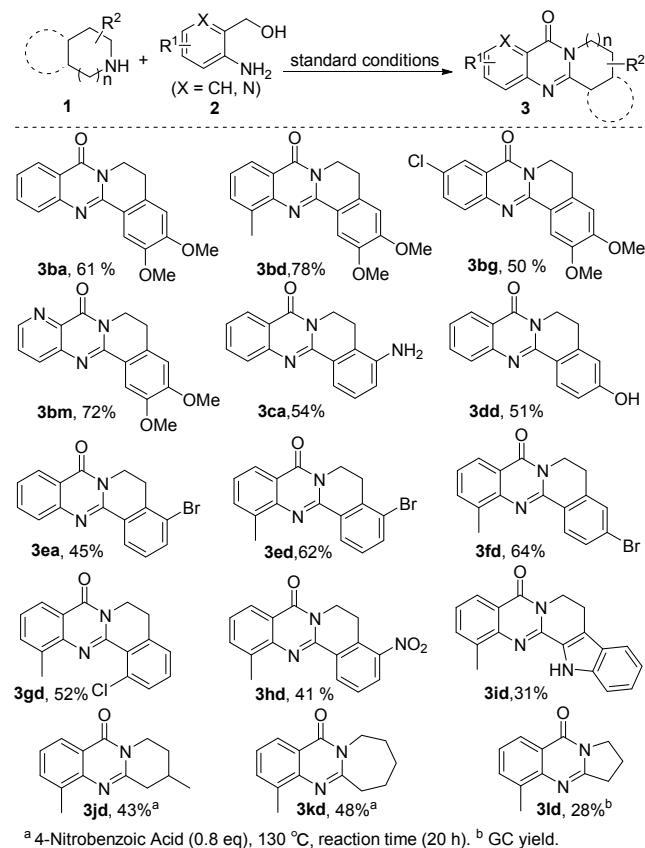
With the nanomaterial prepared, we chose the dehydrogenative cross-coupling of 1,2,3,4-tetrahydroisoquinoline **1a** with 2-aminobenzyl alcohol **2a** as a model reaction to determine an efficient reaction system. The effects of catalysts, acidic additives, solvents, and temperatures were screened (see Table S1 in the SI). An optimal yield (80%) of product **3aa** was acquired at 120 °C in the presence of 1.95 mol% of cobalt catalyst and molecular O₂ by using 4-nitrobenzoic acid as the additive in *p*-xylene (standard conditions). Further, we evaluated the performance of a series of other homogeneous and heterogeneous catalysts, including the cobalt ones (entries 1-8 and 10-15). The results indicated that the use of Co-ZrO₂/N-C (entry 9) is the most suitable choice for the reaction.



Scheme 3. Variation of 2-Aminoarylmethanols

Next, we examined the generality of the synthetic protocol under the optimal conditions. First, the reactions of tetrahydroisoquinoline **1a** with a series of 2-aminoarylmethanols **2** (for structures, see Scheme S1 in SI) were conducted. As shown in Scheme 3, all the reactions proceeded smoothly and furnished desired products in moderate to high yields upon isolation (see **3aa-3an**). The substituents on aryl ring of substrates **2** slightly effect the product formation. Specially, the electron-donating groups enable to afford relatively higher yields (**3ab** and **3ad**) than those of strong electron-withdrawing ones (**3aj** and **3ak**). This

phenomenon is attributed to the electron-rich substituents enhance the -NH₂ nucleophilicity of reactants **2**, thus favoring the coupling step (Scheme 2, from **2** to **3-1**). Interestingly, the 2-aminoheteroarylmethanols (**2i-2n**) were also amenable to the transformation, affording the desired products in moderate to high yields (**3al-3an**).



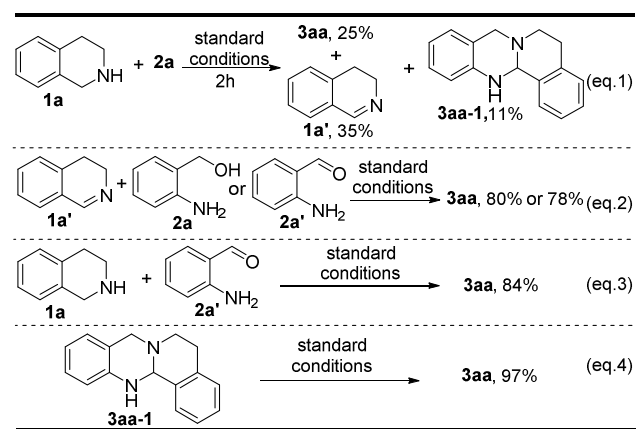
Scheme 4. Both Variations of Two Coupling Partners

Subsequently, we turned our attention to the variation of both coupling partners. As illustrated in Scheme 4, all the reactants underwent smooth dehydrogenative coupling reactions to give the desired products in moderate to good yields. It was found that the cyclic amines have the same substituent effect as 2-aminoarylmethanols **2**. The tetrahydroisoquinolines **1** with electron-donating groups gave higher product yields (**3ba**, **3bd** and **3bm**) than those of electron-deficient ones (**3ea** and **3hd**), which is rationalized as the electron-rich substituents enhance the nucleophilicity of cyclic amines, thus favoring the intramolecular coupling process (Scheme 2, from **3-1** to **3**). Pleasingly, among all the examples tested, we did not observe any by-products arising from the cross-coupling of the amino groups (-NH₂ and -NH) with halogenated substrates (i.e. **2g-2i**, **1e-1g**), indicating that the synthetic protocol proceeds in a chemoselective manner. Moreover, the indole-fused cyclic amine **1i** also reacted with 2-aminobenzyl alcohol **2d**, giving rise to the methylated rutaecarpine product **3id** in 31% yield. Interestingly, the more challenging cyclic amines, such as 4-methylpiperidine (**1j**), azepane (**1k**) and pyrrolidine (**1l**), also could be transformed in combination with **2d** into the ring-size-tunable products in moderate yields (**3jd-3kd**). Noteworthy, a variety of functional groups (i.e. -Me, -OMe, -OH, -CF₃, -NO₂, -NH₂, -F, -Cl and -Br) are well tolerated in the reaction (Scheme 3 and

4), which offers the potential for fabricating complex quinazolinone scaffolds via further chemical transformations.

To examine the reusability of the developed catalyst, five more recyclings were conducted with the model reaction. As shown in Figure S6 (see the SI), we observed a decline of the reaction conversion. Then, after 5 recycling runs, the Co content of catalyst was determined by ICP-AES (0.2 wt%). As shown in Figure S4i, the cobalt elemental mapping of reused catalyst presents relatively weaker signal than the fresh one. So, the decline of catalytic activity is rationalized as the loss of active cobalt species, which results from mechanical abrasion-induced exfoliation during reaction process. The acid leaching experiment (Table S1, entry 22) only resulted in slight loss of catalytic activity. Further, we performed the poisoning experiment,¹⁹ and the addition of KSCN to the model reaction led to a significant decrease of catalyst efficiency (Figure S7). These results in combination with the Co 2p XPS spectrum (Figure S5c) support that the highly dispersed Co-N_x species serve as the catalytic active sites.

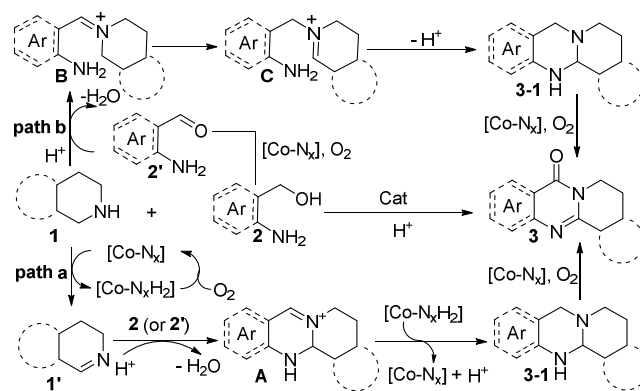
To gain insights into the reaction mechanism, several control experiments were carried out (Scheme 5). First, the model reaction was interrupted after 2 h to analyze the product system. Compound **3aa**, dihydroisoquinoline **1a'** and aminal **3aa-1** were detected in 25%, 35%, 11% yields, respectively (eq.1). Moreover, from the time-concentration profile of the model reaction (Figure S8), aminal **3aa-1** was observed in the whole reaction process and completely consumed after 16 hours. In good agreement with the envisaged protocol (Scheme 2), imine **1a'** was able to couple with **2a** or 2-aminobenzaldehyde **2a'** to afford **3aa** in high yield (eq. 2). Meanwhile, tetrahydroisoquinoline **1a** also reacted with **2a'** to give **3aa** in 84% yield (eq. 3). Treating compound **3aa-1** under the standard conditions generated product **3aa** in almost quantitative yield (eq. 4). These results show that **1a'**, **2a'** and **3aa-1** are the reaction intermediates.



Scheme 5. The Control Experiments

On the basis of the above findings, the possible reaction pathways are depicted in Scheme 6. The cobalt nanocatalyst-induced dehydrogenation of cyclic amine **1** initially forms imine **1'**, which is then trapped by 2-arylaminoethanol **2** or the dehydrogenated aldehyde **2'** to give intermediate **A** via further intramolecular condensation under the assistance of acid. The interaction of **A** with [Co-N_xH₂] species would generate aminals **3-1** (path a). Alternatively, the condensation of cyclic amine **1** with aldehyde **2'** followed by intramolecular nucleophilic addition

also gives aminals **3-1** (path b). Finally, the oxidation of **3-1** would yield the desired product **3**.



Scheme 6. Possible Pathways on Formation of Product 3

In summary, by employing a MOF-templated method, we have developed a highly dispersed and ultralow loading new cobalt nanocatalyst, which has been applied in the first oxidative functionalization of easily available cyclic amines with 2-aminoarylmethanols to ring-fused quinazolinones, the core structures of numerous valuable products. The developed catalytic transformation features broad substrate scope, excellent functional tolerance and chemoselectivity, high step- and atom-efficiency, use of recyclable earth-abundant cobalt catalyst and molecular O₂ as a green oxidant, which offers a practical way for the preparation of quinazolinones with structural diversity. Further applications of the developed nanocobalt to functionalize other inert feedstocks and creation of novel N-heterocyclic systems are currently underway.

ASSOCIATED CONTENT

Supporting Information

The Supporting Information is available free of charge on the ACS Publications website at DOI:

The detail of catalyst preparation, more characterization results, complete experimental procedures and spectral data (PDF)

AUTHOR INFORMATION

Corresponding Author

* minzhang@scut.edu.cn

Notes

The authors declare no competing financial interests.

ACKNOWLEDGMENT

We thank the Science and Technology Program of GuangZhou (201607010306), the Fundamental Research Funds for the Central Universities (2017ZD060), "1000 Youth Talents Plan", Science Foundation for Distinguished Young Scholars of Guangdong (2014A030306018) for financial support.

REFERENCES

- (a) Zhu, Z.; Seidel, D. Acetic Acid Promoted Redox Annulations with Dual C–H Functionalization. *Org. Lett.* **2017**, *19*, 2841–2844. (b) Richers, M. T.; Breugst, M.; Platonova, A. Y.; Ullrich, A.; Dieckmann, A.; Houk, K. N.; Seidel, D. Redox-Neutral α -Oxygenation of Amines: Reaction Development and Elucidation of the Mechanism. *J. Am. Chem. Soc.* **2014**, *136*, 6123–6135. (c) Zhang, C.; De, C. K.; Mal, R.; Seidel, D. α -Amination of Nitrogen Heterocycles: Ring-Fused Aminals. *J. Am. Chem. Soc.* **2008**, *130*, 416–417. (d) Liu, K.; Tang, S.;

- Huang, P.; Lei, A. External Oxidant-Free Electrooxidative [3+2] Annulation between Phenol and Indole Derivatives. *Nat. Commun.* **2017**, *8*, 775.
- (2) Selected examples: (a) Cui, X.; Li, Y.; Bachmann, S.; Scalone, M.; Surkus, A. E.; Junge, K.; Topf, C.; Beller, M. Synthesis and Characterization of Iron-Nitrogen-Doped Graphene/Core-Shell Catalysts: Efficient Oxidative Dehydrogenation of N-Heterocycles. *J. Am. Chem. Soc.* **2015**, *137*, 10652–10658. (b) Chakraborty, S.; Brennessel, W. W.; Jones, W. D. A Molecular Iron Catalyst for the Acceptorless Dehydrogenation and Hydrogenation of N-Heterocycles. *J. Am. Chem. Soc.* **2014**, *136*, 8564–8567.
- (3) (a) Kwon, S. H.; Seo, H. A.; Cheon, C. H. Total Synthesis of Luotonin A and Rutaecarpine from an Aldimine via the Designed Cyclization. *Org. Lett.* **2016**, *18*, 5280–5283. (b) Tseng, M. C.; Yang, H. Y.; Chu, Y. H. Total Synthesis of Asperlicin C, Circumdatin F, Demethylbenzomalvin A, Demethoxycircumdatin H, Sclerotigenin, and Other Fused Quinazolinones. *Org. Biomol. Chem.* **2010**, *8*, 419–427. (c) Bowman, W. R.; Elsegood, M. R. J.; Stein, T.; Weaver, G. W. Radical Reactions with 3*H*-Quinazolin-4-Ones: Synthesis of Deoxyvasicinone, Mackinazolinone, Luotonin A, Rutaecarpine and Tryptanthrin. *Org. Biomol. Chem.* **2007**, *5*, 103–113.
- (4) (a) Fang, J.; Zhou, J. Efficient Syntheses of 2,3-Disubstituted Natural Quinazolinones via Iridium Catalysis. *Org. Biomol. Chem.* **2012**, *10*, 2389–2391. (b) Li, Y.; Feng, T.; Liu, P.; Liu, C.; Wang, X.; Li, D.; Li, N.; Chen, M.; Xu, Y.; Si, S. Optimization of Rutaecarpine as ABCA1 Up-Regulator for Treating Atherosclerosis. *ACS Med. Chem. Lett.* **2014**, *5*, 884–888. (c) Kaur, R.; Manjal, S. K.; Rawal, R. K.; Kumar, K. Recent Synthetic and Medicinal Perspectives of Tryptanthrin. *Bioorg. Med. Chem.* **2017**, *25*, 4533–4552. (d) Liang, J. L.; Cha, H. C.; Jahng, Y. Recent Advances in the Studies on Luotonins. *Molecules* **2011**, *16*, 4861–4883. (e) Rahbæk, L.; Breinholt, J.; Frisvad, J. C.; Christophersen, C. Circumdatin A, B, and C: Three New Benzodiazepine Alkaloids Isolated from a Culture of the Fungus *Aspergillus Ochraceus*. *J. Org. Chem.* **1999**, *64*, 1689–1692.
- (5) Horton, D. A.; Bourne, G. T.; Smythe, M. L. The Combinatorial Synthesis of Bicyclic Privileged Structures or Privileged Substructures. *Chem. Rev.* **2003**, *103*, 893–930.
- (6) Selected examples, see: (a) Wang, Y.; Meng, X.; Chen, G.; Zhao, P. Direct Synthesis of Quinazolinones by Heterogeneous Cu(OH)_x/OMS-2 Catalyst under Oxygen. *Catal. Commun.* **2018**, *104*, 106–111. (b) Zhao, W.; Ma, W.; Xiao, T.; Li, F. Iridium-Catalyzed Cyclization of *o*-Aminobenzamides with Unsaturated Aldehydes to Give 2-Alkylquinazolinones through a Hydrogen Autotransfer Process. *ChemistrySelect* **2017**, *2*, 3608–3612. (c) Li, F.; Lu, L.; Ma, J. Acceptorless Dehydrogenative Condensation of *o*-Aminobenzamides with Aldehydes to Quinazolinones in Water Catalyzed by a Water-Soluble Iridium Complex [Cp*Ir(H₂O)₃][OTf]₂. *Org. Chem. Front.* **2015**, *2*, 1589–1597. (d) Sharif, M.; Opalach, J.; Langer, P.; Beller, M.; Wu, X. F. Oxidative Synthesis of Quinazolinones and Benzothiadiazine 1,1-Dioxides from 2-Aminobenzamide and 2-Aminobenzenesulfonamide with Benzyl Alcohols and Aldehydes. *RSC Adv.* **2014**, *4*, 8–17.
- (7) (a) Shen, C.; Man, N. Y.; Stewart, S.; Wu, X. F. Palladium-Catalyzed Dicarbonylative Synthesis of Tetracycle Quinazolinones. *Org. Biomol. Chem.* **2015**, *13*, 4422–4425. (b) Natte, K.; Neumann, H.; Wu, X. F. Pd/C as an Efficient Heterogeneous Catalyst for Carbonylative Four-Component Synthesis of 4(3*H*)-Quinazolinones. *Catal. Sci. Technol.* **2015**, *5*, 4474–4480. (c) Li, H.; He, L.; Neumann, H.; Beller, M.; Wu, X. F. Cascade Synthesis of Quinazolinones from 2-Aminobenzonitriles and Aryl Bromides via Palladium-Catalyzed Carbonylation Reaction. *Green Chem.* **2014**, *16*, 1336–1343. (d) He, L.; Li, H.; Neumann, H.; Beller, M.; Wu, X. F. Highly Efficient Four-Component Synthesis of 4(3*H*)-Quinazolinones: Palladium-Catalyzed Carbonylative Coupling Reactions. *Angew. Chem., Int. Ed.* **2014**, *53*, 1420–1424. (e) Chen, J.; Natte, K.; Spannenberg, A.; Neumann, H.; Langer, P.; Beller, M.; Wu, X. F. Base-Controlled Selectivity in the Synthesis of Linear and Angular Fused Quinazolinones by a Palladium-Catalyzed Carbonylation/Nucleophilic Aromatic Substitution Sequence. *Angew. Chem., Int. Ed.* **2014**, *53*, 7579–7583. (f) Wu, X. F.; He, L.; Neumann, H.; Beller, M. Palladium-Catalyzed Carbonylative Synthesis of Quinazolinones from 2-Aminobenzamide and Aryl Bromides. *Chem. Eur. J.* **2013**, *19*, 12635–12638. (g) Wu, J.; Zhou, Y.; Wu, T.; Zhou, Y.; Chiang, C. W.; Lei, A. From Ketones, Amines, and Carbon Monoxide to 4-Quinolones: Palladium-Catalyzed Oxidative Carbonylation. *Org. Lett.* **2017**, *19*, 6432–6435.
- (8) Liu, X.; Fu, H.; Jiang, Y.; Zhao, Y. A Simple and Efficient Approach to Quinazolinones under Mild Copper-Catalyzed Conditions. *Angew. Chem., Int. Ed.* **2009**, *48*, 348–351.
- (9) (a) Chen, K.; Gao, B.; Shang, Y.; Du, J.; Gu, Q.; Wang, J. I₂-Catalyzed Cross Dehydrogenative Coupling: Rapid Access to Benzoxazinones and Quinazolinones. *Org. Biomol. Chem.* **2017**, *15*, 8770–8779. (b) Yan, Y.; Xu, Y.; Niu, B.; Xie, H.; Liu, Y.; Yan, Y. I₂-Catalyzed Aerobic Oxidative C(sp³)-H Amination/C-N Cleavage of Tertiary Amine: Synthesis of Quinazolines and Quinazolinones. *J. Org. Chem.* **2015**, *80*, 5581–5587.
- (10) (a) Yamashita, M.; Nishizono, Y.; Himekawa, S.; Iida, A. One-Pot Synthesis of Polyhydroxyprido[1,2-*a*]Indoles and Tetracyclic Quinazolinones from 2-Arylindoles Using Copper-Mediated Oxidative Tandem Reactions. *Tetrahedron* **2016**, *72*, 4123–4131. (b) Feng, Y.; Li, Y.; Cheng, G.; Wang, L.; Cui, X. Copper-Catalyzed Synthesis of 2-Arylquinazolinones from 2-Arylindoles with Amines or Ammoniums. *J. Org. Chem.* **2015**, *80*, 7099–7107. (c) Wang, C.; Zhang, L.; Ren, A.; Lu, P.; Wang, Y. Cu-Catalyzed Synthesis of Tryptanthrin Derivatives from Substituted Indoles. *Org. Lett.* **2013**, *15*, 2982–2985.
- (11) Selected examples, see: (a) Yang, T.; Wang, W.; Wei, D.; Zhang, T.; Han, B.; Yu, W. Synthesis of Quinazolinones via Radical Cyclization of α -Azidyl Benzamides. *Org. Chem. Front.* **2017**, *4*, 421–426. (b) Zheng, J.; Zhang, Y.; Wang, D.; Cui, S. Silver(I)-Mediated Phosphorylation/Cyclization Cascade of N-Cyanamide Alkenes for Divergent Access to Quinazolinones and Dihydroisoquinolinones. *Org. Lett.* **2016**, *18*, 1768–1771. (c) Bao, Y.; Yan, Y.; Xu, K.; Su, J.; Zha, Z.; Wang, Z. Copper-Catalyzed Radical Methylation/C-H Amination/Oxidation Cascade for the Synthesis of Quinazolinones. *J. Org. Chem.* **2015**, *80*, 4736–4742.
- (12) (a) Chen, X. W.; Zhao, H.; Chen, C. L.; Jiang, H. F.; Zhang, M. Hydrogen-Transfer-Mediated α -Functionalization of 1,8-Naphthyridines by a Strategy Overcoming the over-Hydrogenation Barrier. *Angew. Chem., Int. Ed.* **2017**, *56*, 14232–14236. (b) Xie, F.; Xie, R.; Zhang, J. X.; Jiang, H. F.; Du, L.; Zhang, M. Direct Reductive Quinolyl β -C–H Alkylation by Multispherical Cavity Carbon-Supported Cobalt Oxide Nanocatalysts. *ACS Catal.* **2017**, *7*, 4780–4785. (c) Xiong, B.; Jiang, J.; Zhang, S.; Jiang, H.; Ke, Z.; Zhang, M. Ruthenium-Catalyzed Direct Synthesis of Semisaturated Bicyclic Pyrimidines via Selective Transfer Hydrogenation. *Org. Lett.* **2017**, *19*, 2730–2733. (d) Xiong, B.; Zhang, S.; Jiang, H.; Zhang, M. Hydrogen-Transfer-Mediated Direct β -Alkylation of Aryl-1,8-Naphthyridines with Alcohols under Transition Metal Catalyst Free Conditions. *Org. Lett.* **2016**, *18*, 724–727. (e) Xiong, B.; Zhang, S. D.; Chen, L.; Li, B.; Jiang, H. F.; Zhang, M. An Annulative Transfer Hydrogenation Strategy Enables Straightforward Access to Tetrahydro Fused-Pyrazine Derivatives. *Chem. Commun.* **2016**, *52*, 10636–10639. (f) Tan, Z.; Jiang, H.; Zhang, M. A Novel Iridium/Acid Co-Catalyzed Transfer Hydrogenative C(sp³)-H Bond Alkylation to Access Functionalized N-Heteroaromatics. *Chem. Commun.* **2016**, *52*, 9359–9362. (g) Xiong, B.; Li, Y.; Lv, W.; Tan, Z.; Jiang, H.; Zhang, M. Ruthenium-Catalyzed Straightforward Synthesis of 1,2,3,4-Tetrahydronaphthyridines via Selective Transfer Hydrogenation of Pyridyl Ring with Alcohols. *Org. Lett.* **2015**, *17*, 4054–4057. (h) Xie, F.; Zhang, M.; Jiang, H.; Chen, M.; Lv,

- W.; Zheng, A.; Jian, X. Efficient Synthesis of Quinoxalines from 2-Nitroanilines and Vicinal Diols via a Ruthenium-Catalyzed Hydrogen Transfer Strategy. *Green Chem.* **2015**, *17*, 279–284.
- (13) (a) Liang, T.; Tan, Z.; Zhao, H.; Chen, X.; Jiang, H.; Zhang, M. Aerobic Copper-Catalyzed Synthesis of Benzimidazoles from Diaryl- and Alkylamines via Tandem Triple C–H Aminations. *ACS Catal.* **2018**, *8*, 2242–2246. (b) Chen, X.; Zhao, H.; Chen, C.; Jiang, H.; Zhang, M. Iridium-Catalyzed Dehydrogenative α -Functionalization of (Hetero)Aryl-Fused Cyclic Secondary Amines with Indoles. *Org. Lett.* **2018**, *20*, 1171–1174. (c) Tan, Z.; Jiang, H.; Zhang, M. Ruthenium-Catalyzed Dehydrogenative β -Benzoylation of 1,2,3,4-Tetrahydroquinolines with Aryl Aldehydes: Access to Functionalized Quinolines. *Org. Lett.* **2016**, *18*, 3174–3177.
- (14) (a) Zhang, H.; Hwang, S.; Wang, M.; Feng, Z.; Karakalos, S.; Luo, L.; Qiao, Z.; Xie, X.; Wang, C.; Su, D.; Shao, Y.; Wu, G. Single Atomic Iron Catalysts for Oxygen Reduction in Acidic Media: Particle Size Control and Thermal Activation. *J. Am. Chem. Soc.* **2017**, *139*, 14143–14149. (b) Ji, S.; Chen, Y.; Fu, Q.; Chen, Y.; Dong, J.; Chen, W.; Li, Z.; Wang, Y.; Gu, L.; He, W.; Chen, C.; Peng, Q.; Huang, Y.; Duan, X.; Wang, D.; Draxl, C.; Li, Y. Confined Pyrolysis within Metal–Organic Frameworks to Form Uniform Ru₃ Clusters for Efficient Oxidation of Alcohols. *J. Am. Chem. Soc.* **2017**, *139*, 9795–9798. (c) Jagadeesh, R. V.; Murugesan, K.; Alshammari, A. S.; Neumann, H.; Pohl, M.-M.; Radnik, J.; Beller, M. MOF-Derived Cobalt Nanoparticles Catalyze a General Synthesis of Amines. *Science* **2017**, *358*, 326–332. (d) Zhong, W.; Liu, H.; Bai, C.; Liao, S.; Li, Y. Base-Free Oxidation of Alcohols to Esters at Room Temperature and Atmospheric Conditions Using Nanoscale Co-Based Catalysts. *ACS Catal.* **2015**, *5*, 1850–1856. (e) Liu, B.; Zhang, X.; Shioyama, H.; Mukai, T.; Sakai, T.; Xu, Q. Converting Cobalt Oxide Subunits in Cobalt Metal–Organic Framework into Agglomerated Co₃O₄ Nanoparticles as an Electrode Material for Lithium Ion Battery. *J. Power Sources* **2010**, *195*, 857–861.
- (15) (a) Liang, J.; Liang, Z.; Zou, R.; Zhao, Y. Heterogeneous Catalysis in Zeolites, Mesoporous Silica, and Metal–Organic Frameworks. *Adv. Mater.* **2017**, *29*, 1701139. (b) Shen, K.; Chen, X.; Chen, J.; Li, Y. Development of MOF-Derived Carbon-Based Nanomaterials for Efficient Catalysis. *ACS Catal.* **2016**, *6*, 5887–5903. (c) Rimoldi, M.; Howarth, A. J.; DeStefano, M. R.; Lin, L.; Goswami, S.; Li, P.; Hupp, J. T.; Farha, O. K. Catalytic Zirconium/Hafnium-Based Metal–Organic Frameworks. *ACS Catal.* **2016**, *7*, 997–1014. (d) Huang, Z.; Liu, D.; Camacho-Bunquin, J.; Zhang, G.; Yang, D.; López-Encarnación, J. M.; Xu, Y.; Ferrandon, M. S.; Niklas, J.; Poluektov, O. G.; Jellinek, J.; Lei, A.; Bunel, E. E.; Delferro, M. Supported Single-Site Ti (IV) on a Metal–Organic Framework for the Hydroboration of Carbonyl Compounds. *Organometallics* **2017**, *36*, 3921–3930. (e) Zeng, M. H.; Yin, Z.; Tan, Y. X.; Zhang, W. X.; He, Y. P.; Kurmoo, M. Nanoporous Cobalt(II) MOF Exhibiting Four Magnetic Ground States and Changes in Gas Sorption Upon Post-Synthetic Modification. *J. Am. Chem. Soc.* **2014**, *136*, 4680–4688.
- (16) (a) Su, H.; Zhang, K. X.; Zhang, B.; Wang, H. H.; Yu, Q. Y.; Li, X. H.; Antonietti, M.; Chen, J. S. Activating Cobalt Nanoparticles via the Mott–Schottky Effect in Nitrogen-Rich Carbon Shells for Base-Free Aerobic Oxidation of Alcohols to Esters. *J. Am. Chem. Soc.* **2017**, *139*, 811–818. (b) Sahoo, B.; Formenti, D.; Topf, C.; Bachmann, S.; Scalone, M.; Junge, K.; Beller, M. Biomass-Derived Catalysts for Selective Hydrogenation of Nitroarenes. *ChemSusChem* **2017**, *10*, 3035–3039. (c) Han, Y.; Wang, Y. G.; Chen, W.; Xu, R.; Zheng, L.; Zhang, J.; Luo, J.; Shen, R. A.; Zhu, Y.; Cheong, W. C.; Chen, C.; Peng, Q.; Wang, D.; Li, Y. Hollow N-Doped Carbon Spheres with Isolated Cobalt Single Atomic Sites: Superior Electrocatalysts for Oxygen Reduction. *J. Am. Chem. Soc.* **2017**, *139*, 17269–17272. (d) Chen, F.; Sahoo, B.; Kreyenschulte, C.; Lund, H.; Zeng, M.; He, L.; Junge, K.; Beller, M. Selective Cobalt Nanoparticles for Catalytic Transfer Hydrogenation of N-Heteroarenes. *Chem. Sci.* **2017**, *8*, 6239–6246. (e) Schwob, T.; Kempe, R. A Reusable Co Catalyst for the Selective Hydrogenation of Functionalized Nitroarenes and the Direct Synthesis of Imines and Benzimidazoles from Nitroarenes and Aldehydes. *Angew. Chem., Int. Ed.* **2016**, *55*, 15175–15179. (f) Liu, W.; Zhang, L.; Yan, W.; Liu, X.; Yang, X.; Miao, S.; Wang, W.; Wang, A.; Zhang, T. Single-Atom Dispersed Co–N–C Catalyst: Structure Identification and Performance for Hydrogenative Coupling of Nitroarenes. *Chem. Sci.* **2016**, *7*, 5758–5764. (g) Zhang, L.; Wang, A.; Wang, W.; Huang, Y.; Liu, X.; Miao, S.; Liu, J.; Zhang, T. Co–N–C Catalyst for C–C Coupling Reactions: On the Catalytic Performance and Active Sites. *ACS Catal.* **2015**, *5*, 6563–6572.
- (17) Wang, X.; Chen, W.; Zhang, L.; Yao, T.; Liu, W.; Lin, Y.; Ju, H.; Dong, J.; Zheng, L.; Yan, W.; Zheng, X.; Li, Z.; Wang, X.; Yang, J.; He, D.; Wang, Y.; Deng, Z.; Wu, Y.; Li, Y. Uncoordinated Amine Groups of Metal–Organic Frameworks to Anchor Single Ru Sites as Chemoselective Catalysts toward the Hydrogenation of Quinoline. *J. Am. Chem. Soc.* **2017**, *139*, 9419–9422.
- (18) (a) Cao, Y.; Mao, S.; Li, M.; Chen, Y.; Wang, Y. Metal/Porous Carbon Composites for Heterogeneous Catalysis: Old Catalysts with Improved Performance Promoted by N-Doping. *ACS Catal.* **2017**, *7*, 8090–8112. (b) Yang, C.; Fu, L.; Zhu, R.; Liu, Z. Influence of Cobalt Species on the Catalytic Performance of Co–N–C/SiO₂ for Ethylbenzene Oxidation. *Phys. Chem. Chem. Phys.* **2016**, *18*, 4635–4642. (c) He, L.; Weniger, F.; Neumann, H.; Beller, M. Synthesis, Characterization, and Application of Metal Nanoparticles Supported on Nitrogen-Doped Carbon: Catalysis beyond Electrochemistry. *Angew. Chem., Int. Ed.* **2016**, *55*, 12582–12594. (d) Sushkevich, V. L.; Ivanova, I. I.; Taarning, E. Ethanol Conversion into Butadiene over Zr-Containing Molecular Sieves Doped with Silver. *Green Chem.* **2015**, *17*, 2552–2559.
- (19) (a) Tang, C.; Surkus, A. E.; Chen, F.; Pohl, M. M.; Agostini, G.; Schneider, M.; Junge, H.; Beller, M. A Stable Nanocobalt Catalyst with Highly Dispersed CoN_x Active Sites for the Selective Dehydrogenation of Formic Acid. *Angew. Chem., Int. Ed.* **2017**, *56*, 16616–16620. (b) Singh, D.; Mamtani, K.; Bruening, C. R.; Miller, J. T.; Ozkan, U. S. Use of H₂S to Probe the Active Sites in FeNC Catalysts for the Oxygen Reduction Reaction (ORR) in Acidic Media. *ACS Catal.* **2014**, *4*, 3454–3462. (c) Zhang, X.; Lu, P.; Cui, X.; Chen, L.; Zhang, C.; Li, M.; Xu, Y.; Shi, J. Probing the Electro-Catalytic ORR Activity of Cobalt-Incorporated Nitrogen-Doped CNTs. *J. Catal.* **2016**, *344*, 455–464.

